Renormalization of the H-point phonon anomaly in molybdenum

C.-L. Fu, K.-M. Ho, and B. N. Harmon
Ames Laboratory, U. S. Department of Energy, Ames, Iowa 50011
and Department of Physics, Iowa State University, Ames, Iowa 50011

S. H. Liu
Solid State Division, Oak Ridge National Laboratory, Oak Ridge, Tennessee 37830
(Received 5 May 1983)

The frequency of the H-point phonon of molybdenum obtained from precise frozen-phonon calculations differs from the experimental value by 9%. An analysis of this unusually large discrepancy shows that nonadiabatic effects are small, while effects caused by the many-body renormalization of electronic states near the Fermi energy are of the same order of magnitude as the discrepancy.

Frozen-phonon calculations provide an accurate first-principles approach for the study of lattice dynamics. The calculations (with no adjustable parameters) involve the precise evaluation of the total electronic energy of a crystal lattice which has been distorted by atomic displacements corresponding to a particular phonon mode. From the curve of total energy versus lattice displacement one may obtain the phonon frequency as well as information about anharmonic effects and lattice instabilities. The method has been demonstrated for semiconductors and yields phonon frequencies accurate to within a few percent.[1-5] We have recently applied the method to transition metals using a self-consistent pseudopotential approach within the local density formalism to evaluate the total electronic energy.[6] We obtained excellent agreement with experiment for the equilibrium structural properties (e.g., the lattice constant and bulk modulus) of Nb and Mo and were able to show that at low temperatures the bcc phase of Zr is unstable with respect to ω-phase transformation. For phonon frequencies we made extensive tests of precision and convergence and found that, except for the H-point phonon in Mo, the agreement with experiment was always within the experimental and theoretical error limits ($\sim 2\%$). The 9% discrepancy for the Mo H-point phonon amounts to a 0.5-THz difference in frequency. This is larger than we would expect from the numerical precision of the calculations and the quoted experimental uncertainty. To investigate possible causes for the discrepancy we have studied the approximations which are assumed in the frozen-phonon method and have examined the conditions under which there might be problems with these approximations. In particular we have estimated the frequency shifts caused by nonadiabatic effects which we find to be negligible and many-body renormalization effects which we find to be significant.

The main differences between the Mo H-point phonon and the other phonons we have investigated is that this phonon is associated with a Kohn anomaly arising from the well-known nesting feature of the energy bands near the Fermi level.[7] In isoelectronic Cr this same nesting feature gives rise to a spin-density wave with a wave vector near H. In Mo, this causes a sharp dip in the phonon dispersion curves at the H point.[8] Measurements of the phonon dispersion curves as a function of temperature[9] show that this dip diminishes at high temperature indicating the importance of contributions of states near the Fermi level to the phonon frequency at the H point. An analysis of the distorted band structure corresponding to the H-point phonon confirms that the anomaly is caused by large band splittings occurring at the Fermi level. The frozen-phonon method relies on the adiabatic approximation which neglects the time dependence of the ionic motions. Since the adiabatic approximation is suspect when Fermi-surface nesting features occur in the electronic band structure,[10,11] we investigated the possible breakdown of this approximation. Another correction we have studied is the renormalization of electronic states near the Fermi level by excitation of virtual phonon modes [shown schematically in Fig. 1(c)]. Before giving our numerical results we will briefly discuss each of these corrections.

According to standard lattice-dynamical theory,[12] the electronic contribution to the phonon frequency due to the electron-phonon (e-ph) interaction is given to lowest order by the real part of the diagram shown in Fig. 1(b). In the random-phase approximation, this contribution can be represented in abbreviated notation by

$$\omega^{e\text{-ph}}=(g^0\underline{\epsilon}^{-1})^\dagger\underline{\chi}^0 g^0 , \tag{1}$$

where $\underline{\chi}^0$ is the electronic susceptibility, g^0 is the scattering matrix element between electronic states due to the e-ph interaction, and $\underline{\epsilon}=\underline{1}-v_c\underline{\chi}^0$ is the dielectric matrix of the electron system which includes the screening due to the electrons. Following Refs. 7 and 12, Eq. (1) can be regrouped into two terms which can be written as

$$\omega^{e\text{-ph}}=(g^0\underline{\epsilon}^{-1})^\dagger\underline{\chi}^0(\underline{\epsilon}^{-1}g^0)-(g^0\underline{\chi})^\dagger v_c(\underline{\chi}\,g^0) , \tag{2}$$

where v_c is the Coulomb interaction between electrons including exchange-correlation energy and $\underline{\chi}=\underline{\chi}^0/\underline{\epsilon}^{-1}$. The second term may be interpreted as a contribution from

charge distortions caused by the phonon whereas the first term represents a band-structure contribution.[12] Since we are interested in the effects of band splitting near the Fermi level, in the following we will concentrate on the first term.

For most cases, the effect of renormalization on phonon frequencies is negligible and it is a good approximation to replace the dressed electron propagator in Fig. 1(b) by the bare propagator. However, when the electronic response contains a large contribution from electrons whose energies are in the range of the Debye energy (ω_D) of the Fermi level, the dressing effects due to the phonon cloud become important.[13] Taking into account this "renormalization" effect on the electrons [Fig. 1(c)], the band-structure contribution to the phonon self-energy obtained from Dyson's equation and shown diagramatically in Fig. 1(b) can be written in terms of temperature Green's function as

$$\pi_{\vec{q}} = T \sum_{\epsilon} \sum_{\vec{k}} |g^s(\vec{q},\vec{k})|^2 G(\vec{k}-\vec{q},\epsilon-\omega_{\vec{q}}) G(\vec{k},\epsilon) \ . \tag{3}$$

The real part of $\pi_{\vec{q}}$ represents the phonon-frequency shift. Following Ref. 14, it is given by

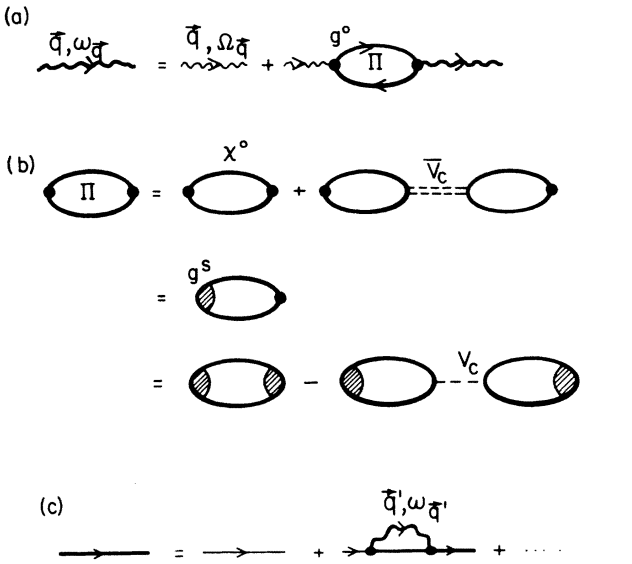

FIG. 1. (a) Dyson equation for the phonon propagator in the electron-phonon system. The heavy and light wavy lines represent the bare and normalized phonon propagator, respectively, g^0 is the bare e-ph interaction, and Π is the proper phonon self-energy. (b) Equations (1) and (2) in diagrammatic form. The heavy line is the dressed electron propagator, $\bar{v}_c$ and v_c represent the screened and bare Coulomb interaction, respectively, and g^s is the screened vertex. (c) Electron propagator with phonon renormalization.

$$\mathrm{Re}\pi_{\vec{q}} = \frac{1}{2\pi} \int_{-\infty}^{\infty} d\epsilon \sum_{\vec{k}} |g^s(\vec{q},\vec{k})|^2 [\mathrm{Im}G_R(\vec{k},\epsilon)\mathrm{Re}G_R(\vec{k}-\vec{q},\epsilon-\omega_{\vec{q}}) + \mathrm{Im}G_R(\vec{k}-\vec{q},\epsilon)\mathrm{Re}G_R(\vec{k},\epsilon+\omega_{\vec{q}})] \tanh\frac{\epsilon}{2T} \ . \tag{4}$$

In Eqs. (3) and (4), g^s is the screened e-ph matrix element, and $\omega_{\vec{q}}$ is the phonon frequency. For electronic states with energies far from the Fermi level, the replacement of G_R by the bare propagator has a negligible effect. However, when the bare electronic energies, $E^0_{\vec{k}}$ and $E^0_{\vec{k}-\vec{q}}$, are within the range of ω_D from the Fermi level, there is a rapid variation of the electron self-energy, Σ, and the electron Green's function can be expressed as

$$G_R(\vec{k},\epsilon) = \frac{Z_{\vec{k}}}{\epsilon - \tilde{E}_{\vec{k}} + i\delta\,\mathrm{sgn}(k-k_f)}, \quad \delta \to 0^+ \ , \tag{5}$$

where $\tilde{E}_{\vec{k}} = Z_{\vec{k}} E^0_{\vec{k}}$,

$$Z_{\vec{k}} = \left[1 - \frac{d\Sigma(\epsilon)}{d\epsilon}\bigg|_{\epsilon=\tilde{E}_{\vec{k}}} \right]^{-1} \equiv (1+\lambda)^{-1} \ ,$$

where λ is the usual e-ph coupling constant.

Substituting Eq. (5) into (4), we find that the Fermi-surface (FS) contribution to $\mathrm{Re}\pi_{\vec{q}}$ is given by

$$\begin{aligned} \omega^{e\text{-ph}}_{\vec{q}} &\simeq \sum_{\vec{k}}^{(\mathrm{FS})} \frac{Z^2 |g^s(\vec{q},\vec{k})|^2 (f^0_{\vec{k}} - f^0_{\vec{k}-\vec{q}})}{\tilde{E}_{\vec{k}} - \tilde{E}_{\vec{k}-\vec{q}} - \omega_{\vec{q}}} \\ &= \frac{1}{1+\lambda} \sum_{\vec{k}}^{(\mathrm{FS})} \frac{|g^s(\vec{q},\vec{k})|^2 (f^0_{\vec{k}} - f^0_{\vec{k}-\vec{q}})}{E^0_{\vec{k}} - E^0_{\vec{k}-\vec{q}} - \omega_{\vec{q}}(1+\lambda)} \\ &\simeq \frac{1}{1+\lambda} \sum_{\vec{k}}^{(\mathrm{FS})} \frac{|g^s(\vec{q},\vec{k})|^2 (f^0_{\vec{k}} - f^0_{\vec{k}\vec{q}})}{E^0_{\vec{k}} - E^0_{\vec{k}-\vec{q}}} \ , \end{aligned} \tag{6}$$

which is reduced by a factor $(1+\lambda)$ from the expression obtained without considering the renormalization. The last step is justified only when the correction for the time dependence of the ionic motion is small. The summation in Eq. (6) is over the region of Brillouin zone where E^0's are of the order ω_D from the Fermi level.

In the frozen-phonon calculations only one phonon mode is present and the renormalization effect due to the virtual phonons which give rise to the $1/(1+\lambda)$ factor is missing. Thus the frozen-phonon calculations overestimate the effect of the Fermi-surface band splitting and should have a correction given by

$$\Delta\omega(\text{ren}) \cong \frac{-\lambda}{1+\lambda} \sum_{\vec{k}} \frac{|g^s(\vec{k},\vec{q})|^2 (f^0_{\vec{k}} - f^0_{\vec{k}+\vec{q}})}{E^0_{\vec{k}} - E^0_{\vec{k}+\vec{q}}} . \quad (7)$$

where (ren) indicates the renormalization effect.

The $(1+\lambda)$ factor has a simple origin. In the frozen-phonon calculation, the contribution to $\omega^{e\text{-ph}}_{\vec{q}}$ is given symbolically as $-\tilde{N}(0)|g^s|^2$, where $\tilde{N}(0)$ is the portion of density of states at the Fermi level affected by band splittings. The inclusion of the virtual phonon processes renormalize the electronic states near the Fermi level. This effect will be reflected in the enhancement of the density of states and the reduction of the scattering matrix elements. Thus in symbolic form

$$\tilde{N}(0)|g^s|^2 \rightarrow (1+\lambda)\tilde{N}(0)\frac{1}{(1+\lambda)^2}|g^s|^2 = \frac{1}{1+\lambda}\tilde{N}(0)|g^s|^2 ,$$

where the arrow indicates phonon renormalization.

The correction due to the time dependence of the ionic motions has previously been investigated in detail and is given by[10,11]

$$\Delta\omega(\text{adi}) = \sum_{\vec{k}} |g^s(\vec{k},\vec{q})|^2 (f^0_{\vec{k}} - f^0_{\vec{k}+\vec{q}}) \times \left[\frac{1}{E^0_{\vec{k}} - E^0_{\vec{k}+\vec{q}} + \omega_{\vec{q}}} - \frac{1}{E^0_{\vec{k}} - E^0_{\vec{k}+\vec{q}}} \right] , \quad (8)$$

where (adi) indicates the adiabatic effects.

Since both corrections involve electron states in a very narrow energy region about the Fermi energy, we can simplify the evaluation of Eqs. (7) and (8) by parametrizing our first-principles band structure by the velocities and deviations from perfect nesting of the bands at the Fermi level. We can also obtain the fully screened electron-phonon matrix elements ($\underline{\epsilon}^{-1}g^0$) for the bands of interest from the band splittings in our frozen-phonon calculations. Using these procedures, we estimated the contribution from states near the Fermi level and the corrections that must be applied to the frozen-phonon results for the Mo H-point phonon (see Appendix A for details). We find that the $\Delta\omega$(adi) correction is very small (amounting to less than 2% of the Fermi-surface contribution to the Kohn anomaly) even though the nesting occurs in a relatively large portion of the Brillouin zone. However, the correction $\Delta\omega$(ren) is not negligible. If we include only contributions from bands within five ω_D of the Fermi level, we obtain a depression of the H-phonon frequency by 0.8 THz.[15] According to our theory above, this contribution is overestimated in the frozen-phonon calculation, and inclusion of phonon renormalization effects will cause a reduction in the size of the dip by a factor of $1/(1+\lambda)$ [for Mo, $\lambda \cong 0.47$].[16] Taking this correction into account, we find that the frequency of the H phonon as obtained from the frozen-phonon calculations should be increased by 0.25 ± 0.1 THz. The renormalization correction is in the right direction to account for the discrepancy between our original theoretical result of 5.0 ± 0.1 THz and the experimental result of 5.5 ± 0.1 THz.[8,9] Our method of estimating the renormalization effect is of course approximate and only indicates the magnitude and direction of the effect. The actual pieces of the Fermi surface responsible for the Kohn anomaly may have a λ value which differs from the average, and more precise calculations would treat the electron-phonon matrix elements explicitly rather than assuming a constant value.

Since phonon renormalization affects only energy bands in a very narrow energy range near the Fermi level, its effect on the phonon frequency can be neglected except in the case of a phonon anomaly where there is an appreciable contribution from electronic states right at the Fermi level. For this case renormalization is a significant effect which is not included in frozen-phonon calculations. It is interesting to note that there are no corresponding effects of renormalization on the phonon linewidth (see Appendix B for details).

ACKNOWLEDGMENTS

We would like to thank Professor C. Stassis and Professor H. Rietschel for valuable discussions. We are also grateful to Professor P. Allen for pointing out the steps in the derivation for the phonon linewidth. Ames Laboratory is operated for the U.S. Department of Energy by Iowa State University under contract No. W-7405-Eng-82. Oak Ridge National Laboratory is operated by the Union Carbide Corporation for the U.S. Department of Energy under Contract No. W-7405-Eng-82. This work was supported by the Director of Energy Research, Office of Basic Energy Sciences.

APPENDIX A

In this appendix, we will give the details on the evaluation of Eqs. (7) and (8). For the Mo H-point phonon, the phonon anomaly is caused by the nesting bands (labeled as 1 and 2 in the following) near the Fermi level. The Fermi-surface contribution to the phonon frequency without renormalization can be rewritten as

$$\omega^{e\text{-ph}}_{\vec{q}} = \sum_{\vec{k}}^{(\text{FS})} |g^s(\vec{q},\vec{k})|^2 \frac{f^0_{1,\vec{k}}(1-f^0_{2,\vec{k}+\vec{q}})}{E^0_{1,\vec{k}} - E^0_{2,\vec{k}+\vec{q}} + \omega_{\vec{q}}} + \frac{f^0_{2,\vec{k}}(1-f^0_{1,\vec{k}-\vec{q}})}{E^0_{2,\vec{k}} - E^0_{1,\vec{k}-\vec{q}} - \omega_{\vec{q}}} . \quad (A1)$$

The adiabatic approximation corresponds to setting $\omega_{\vec{q}} = 0$ in Eq. (B1).

Since we are only interested in a narrow energy range around the Fermi level, we can assume linear bands in the z direction:

$$E^0_{1,\vec{k}} = -V_1(k_z - k_f) ,$$

and (A2)

$$E^0_{2,\vec{k}} = V_2(k_z - k_f - Q) ,$$

where the linear velocities V's and the nesting wave vector Q are functions of k_x and k_y. The z direction is along the $\vec{q}$ vector which is equal to $(0,0,2\pi/a)$ for the H-point phonon.

The e-ph matrix elements can be obtained from the magnitude of the band splittings in the frozen-phonon calculation. For an atomic displacement of $\sim 2\%$ of the lattice constant, we obtained splittings around the Fermi level ranging from 0.55 to 0.65 eV. Therefore, it is a good approximation to assume constant matrix elements over the Fermi surface to simplify the calculation. Also we found that the linear velocities V's are essentially independent of k_x and k_y in the region of interest, thus constant velocities have been used. Integration over k_z in Eq. (A1) gives

$$\omega_{\vec{q}}^{e\text{-ph}} \simeq -\frac{|g^s|^2}{V_1+V_2}\frac{\Omega}{4\pi^3}\int dk_x dk_y \ln\left|\frac{(V_1+V_2)^2(\Delta K_z)}{[V_1(q-Q)+\omega_q][V_2(q-Q)-\omega_q]}\right| . \tag{A3}$$

ΔK_z in Eq. (A3) represents the region where E_1^0 and E_2^0 are of the order of several ω_D from the Fermi level. However, the exact choice of ΔK_z is not critical since the contribution to the integral goes as $\ln(\Delta K_z)$ which changes slowly with ΔK_z. The first-principles band calculations indicate that the nesting vector Q can be well parametrized over the region of interest by the expression

$$Q = a + b(k_x - k_x^0)^2 , \tag{A4}$$

where a is a function of k_y; k_x^0 and b are constant.

Substituting Eq. (A4) into (A3), we can do the integration over k_x analytically; it is then easy to perform the remaining integral over k_y numerically.

APPENDIX B

In this appendix the effect on phonon linewidth caused by the renormalization of the electronic states near the Fermi level are derived with the methods of many-body theory.

The phonon linewidth due to e-ph interaction is expressed as[17]

$$\delta_{\vec{q}} = \lim_{\xi\to 0}\frac{\omega_{\vec{q}}\,\mathrm{Im}\Pi_{\vec{q}}(\xi)}{\xi} . \tag{B1}$$

In analogy to the $\mathrm{Re}\Pi_{\vec{q}}$ already discussed, the imaginary part is given by[18]

$$\mathrm{Im}\Pi_{\vec{q}}(\xi) = \frac{\pi}{1+\lambda}\sum_{\vec{k}} |g^s(\vec{q},\vec{k})|^2 (f^0_{\vec{k}} - f^0_{\vec{k}-\vec{q}})\delta(E^0_{\vec{k}} - E^0_{\vec{k}-\vec{q}} - \xi(1+\lambda)) \quad \text{for } \xi \le \omega_D . \tag{B2}$$

If we introduce a factor

$$1 = \int d\epsilon\,\delta(\epsilon - E^0_{\vec{k}}) \int d\epsilon'\,\delta(\epsilon' - E^0_{\vec{k}-\vec{q}})$$

into the integrand of Eq. (B2), and define

$$[N(0)]^2 I^2(\epsilon,\epsilon') \equiv \sum_{\vec{k}} |g^s(\vec{q},\vec{k})|^2 \delta(\epsilon - E^0_{\vec{k}}) \times \delta(\epsilon' - E^0_{\vec{k}-\vec{q}}) , \tag{B3}$$

then Eq. (B2) can be written as

$$\mathrm{Im}\Pi_{\vec{q}}(\xi) = \frac{\pi}{1+\lambda}\int d\epsilon\, d\epsilon' [N(0)]^2 |I(\epsilon,\epsilon')|^2 \times [f^0(\epsilon) - f^0(\epsilon')] \times \delta(\epsilon - \epsilon' - \xi(1+\lambda)) . \tag{B4}$$

For $\xi \to 0$, $I^2(\epsilon,\epsilon')$ in Eq. (B4) varies slowly with ϵ and ϵ' (compared with the other (ϵ,ϵ') dependent factors remaining in the $\int d\epsilon\, d\epsilon'$ integrals). Therefore we can replace $I^2(\epsilon,\epsilon')$ by $I^2(0,0) \equiv \langle I^2_{\vec{q}} \rangle$. Thus Eq. (B4) becomes

$$\begin{aligned}\lim_{\xi\to 0}\mathrm{Im}\,\Pi_{\vec{q}}(\xi) &= \frac{\pi}{1+\lambda}[N(0)]^2\langle I^2_{\vec{q}}\rangle \times \int d\epsilon [f^0(\epsilon) - f^0(\epsilon + \xi(1+\lambda))] \\ &= \frac{\pi}{1+\lambda}[N(0)]^2\langle I^2_{\vec{q}}\rangle (1+\lambda)\xi \\ &= \pi[N(0)]^2\langle I^2_{\vec{q}}\rangle \xi . \end{aligned} \tag{B5}$$

Substituting (B5) into (B1), the phonon linewidth is then given by

$$\delta_{\vec{q}} = \pi\omega_{\vec{q}}[N(0)]^2\langle I^2_{\vec{q}}\rangle , \tag{B6}$$

which is identical to the expression obtained without considering the renormalization effect.[19]

[1] M. T. Yin and M. L. Cohen, Phys. Rev. Lett. 45, 1004 (1980).

[2] J. Ihm, M. T. Yin, and M. L. Cohen, Solid State Commun. 37, 491 (1981).

[3] H. Wendel and R. M. Martin, Phys. Rev. Lett. 40, 950 (1978); Phys. Rev. B 19, 5251 (1979).

[4] B. N. Harmon, W. Weber, and D. R. Hamann, Phys. Rev. B 25, 1109 (1982).

[5] K. Kunc and R. M. Martin, Phys. Rev. Lett. 48, 406 (1982).

[6] K. M. Ho, C. L. Fu, B. N. Harmon, W. Weber, and D. R. Hamann, Phys. Rev. Lett. 49, 673 (1982).

[7]C. M. Varma and W. Weber, Phys. Rev. B 19, 6142 (1979).
[8]B. M. Powell, P. Martel, and A. D. B. Woods, Phys. Rev. 171, 727 (1968); W. J. L. Buyers, B. M. Powell, and A. D. B. Woods, Can. J. Phys. 50, 3069 (1972).
[9]J. Zarestky, C. Stassis, B. N. Harmon, K.-M. Ho, and C. L. Fu, Phys. Rev. B 28, 697 (1983).
[10]G. V. Chester, Adv. Phys. 10, 357 (1961).
[11]E. G. Brovman and Yu. Kagan, Zh. Eksp. Teor. Fiz. 52, 557 (1967) [Sov. Phys.—JETP 25, 365 (1967)].
[12]See the review by P. B. Allen, in *Dynamical Properties in Solids,* edited by G. K. Horton and A. A. Maradudin (North-Holland, Amsterdam, 1979), Vol. III, p. 97.
[13]D. J. Scalapino, in *Superconductivity,* edited by R. D. Parks (Dekker, New York, 1969), Vol. I, p. 449.
[14]A. A. Abrikosov, L. P. Gor'kov, and I. E. Dzyaloshinski, *Methods of Quantum Field Theory in Statistical Physics* (Dover, New York, 1975), p. 178.
[15]The choice of cutoff energy is not very critical, since the main contribution ($\sim 50\%$) to the summation of Eq. (4) comes from energies within ω_D of the Fermi level.
[16]B. Chakraborty, W. E. Pickett, and P. B. Allen, Phys. Rev. B 14, 3227 (1976).
[17]T. Holstein, Ann. Phys. (N.Y.) 29, 410 (1964).
[18]Only the first diagram in the bottom line of Fig. 1(b) contributes to the imaginary part.
[19]W. H. Butler, F. J. Pinski, and P. B. Allen, Phys. Rev. B 19, 3708 (1978).